

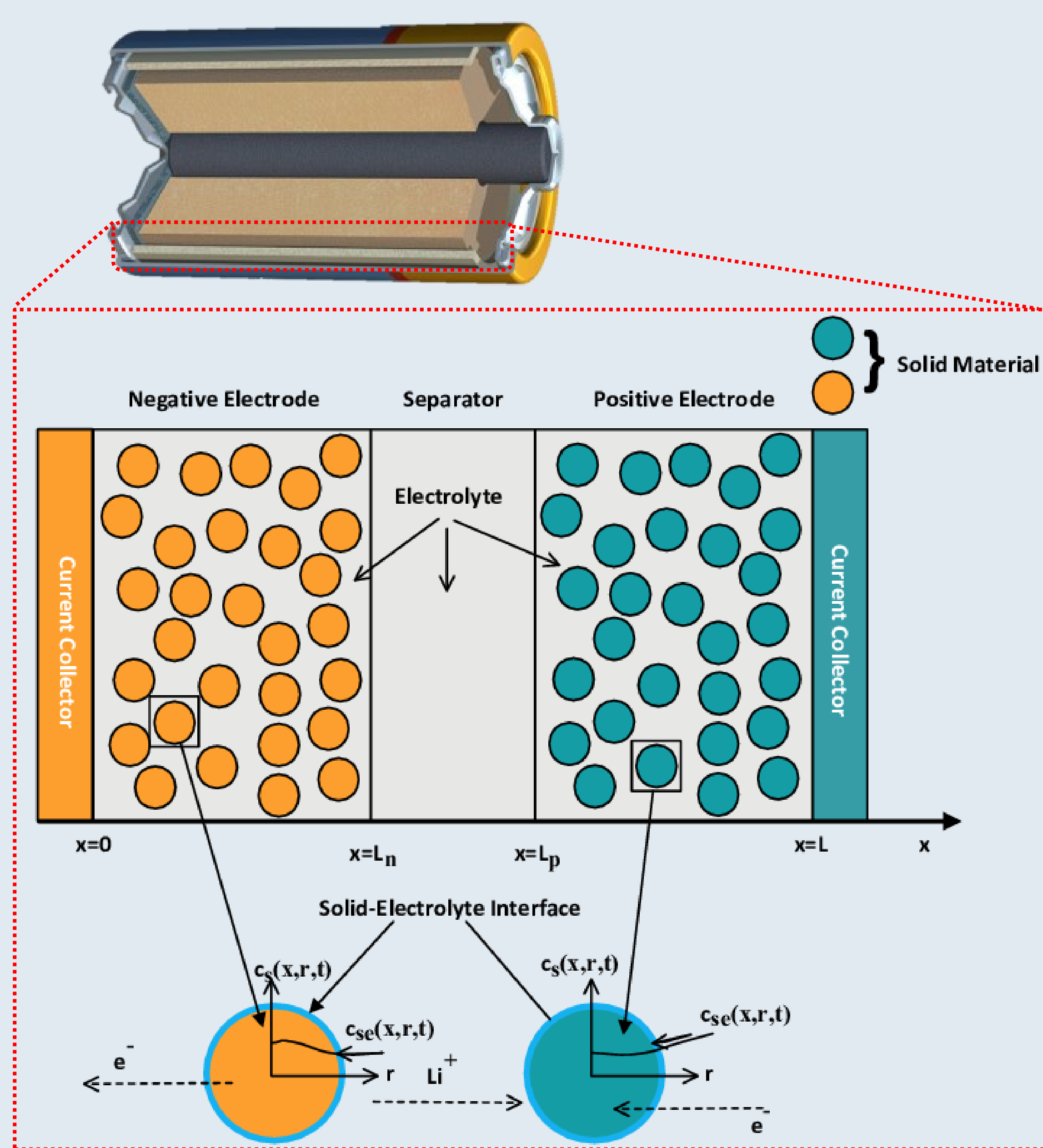
Physics-Based Modeling of Lithium Plating on Graphite Anode of Commercial Lithium-Ion Batteries

Modeling lithium plating in 18650 Lithium-ion battery cells to understand its impact on cell degradation and safety and develop optimal fast charging protocols.

Sina Navidi¹, Benjamin Nowacki¹, Aidan Lawlor¹, Jun Xu², Chao Hu¹

1. School of Mechanical, Aerospace, and Manufacturing Engineering, University of Connecticut, Storrs, CT, USA

2. Department of Mechanical Engineering, University of Delaware, Newark, DE, USA



Abstract

Lithium plating on the graphite anode significantly contributes to the degradation of cell capacity, initiation of internal short circuits, and escalation of thermal runaway in lithium-ion batteries. Non-intrusive detection methods for lithium plating are critical for the safe and reliable operation of lithium-ion batteries. This study presents a physics-based pseudo-two-dimensional (P2D) model that incorporates lithium plating and stripping reactions to describe the electrochemical behavior of commercial 18650 cylindrical cells with graphite and LiFePO₄ (LFP) electrodes at high current rates and low temperatures.

Simulations were performed using COMSOL MULTIPHYSICS 6.1, and the results were compared with experimental measurements obtained from a Neware CT-4000 series battery testing system. The voltage response and surface temperature of 48 commercial 18650 LFP cells at varying states of health (100% to 75% at an approximately 5% increment) and charge (100% to 0% at an approximately 5% increment) were collected. These results can inform the establishment of operational and design limits to mitigate capacity degradation and safety hazards inherent in these cells.

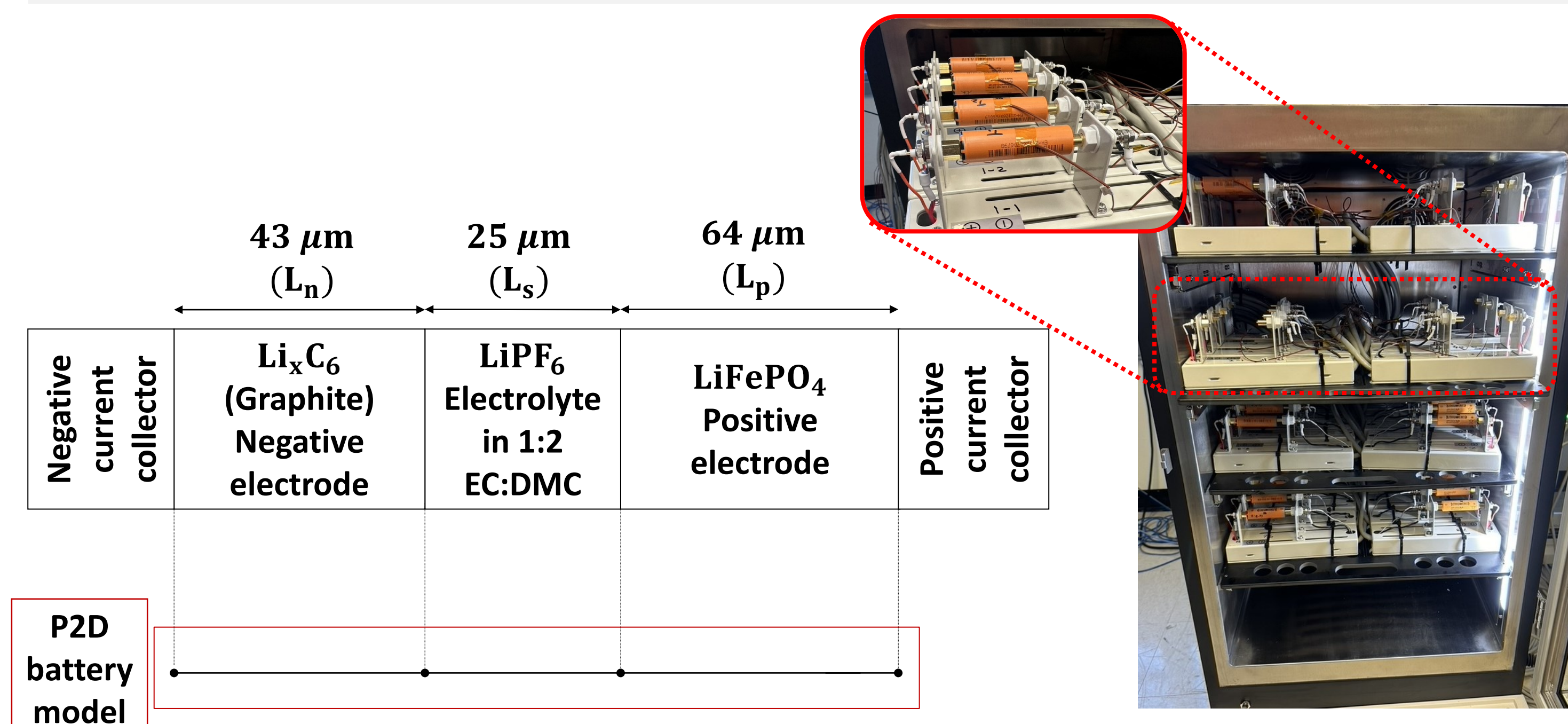


FIGURE 1. Left: Schematic of the electrochemical P2D model. Right: Experimental setup for validation.

Methodology

A P2D model is developed for the LFP-graphite 18650 cell, incorporating lithium plating and stripping reactions as detailed in the table below.

Process	Reaction	Current (A/m ²)	Kinetics Equations
Intercalation	$\text{Li}_x\text{C}_6 + \Delta x \text{Li}^+ + e^- \rightarrow \text{Li}_{x+\Delta x}\text{C}_6$	j_1	$j_1 = i_{0,1} \left[\exp\left(\frac{\alpha_{a,1} F \eta_1}{RT}\right) - \exp\left(\frac{\alpha_{c,1} F \eta_1}{RT}\right) \right]$ <ul style="list-style-type: none"> $i_{0,1} = k_1 \cdot c_e^{\alpha_{a,1}} (c_{s,\text{max}} - c_{s,\text{surf}})^{\alpha_{a,1}} c_{s,\text{surf}}^{\alpha_{c,1}}$ $\eta_1 = \phi_s - \phi_e - U - FjR_{\text{SEI}}$ $U = U_{\text{ref}}(x) - (T - T_{\text{ref}}) \left(\frac{dU}{dT}\right)$ $R_{\text{SEI}} = (\delta_{\text{SEI},0} + \Delta\delta_{\text{SEI}}) / \sigma_{\text{SEI}}$
Plating	$\text{Li}^+ + e^- \rightarrow z_1 \text{Li}_{\text{rev}}^{(s)} + z_2 \text{Li}_{\text{dead}}^{(s)} + z_3 \text{SEI}$	j_2	$j_2 = i_{0,2} \left[\exp\left(\frac{\alpha_{a,2} F \eta_{\text{Li}}}{RT}\right) - \exp\left(\frac{\alpha_{c,2} F \eta_{\text{Li}}}{RT}\right) \right], \eta_{\text{Li}} < 0$ <ul style="list-style-type: none"> $i_{0,2} = k_2 \cdot c_e^{\alpha_{a,2}}$ $\eta_{\text{Li}} = \phi_s - \phi_e - U_{\text{Li}} - FjR_{\text{SEI}}$
Stripping	$\text{Li}^{(s)} \rightarrow \text{Li}^+ + e^-$	j_3	$j_3 = i_{0,2} \left[\exp\left(\frac{\alpha_{a,2} F \eta_{\text{Li}}}{RT}\right) - \exp\left(\frac{\alpha_{c,2} F \eta_{\text{Li}}}{RT}\right) \right] \cdot \left(\frac{\beta \cdot \eta_{\text{Li,rev}}}{1 + \beta \cdot \eta_{\text{Li,rev}}} \right), \eta_{\text{Li}} > 0, \eta_{\text{Li,rev}} > 0$

Results

The results can be seen in Figure 2, which shows the anode overpotential alongside the lithium plating current and the corresponding changes in lithium film thickness on both the separator and the current collector. The model highlights the dynamics of lithium plating under the given operating conditions (C-rates), revealing how the anode potential influences the onset and progression of lithium deposition. The variations in lithium film thickness indicate the spatial distribution of plating across the anode, with significant changes occurring at both the separator and current collector interfaces.

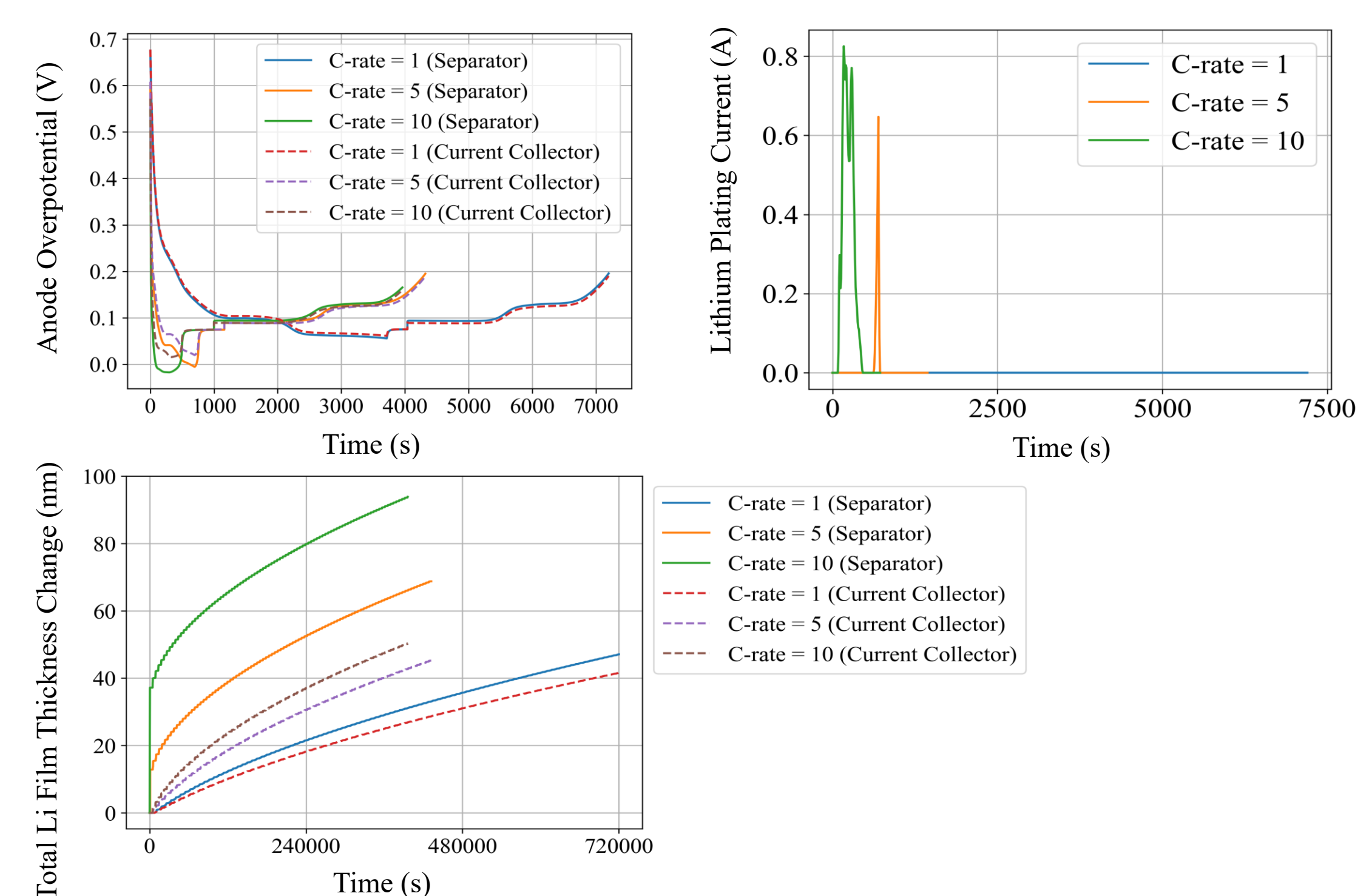


FIGURE 2. Simulation results from the P2D model showing anode overpotential, lithium plating current, and change in lithium film thickness on both the separator and current collector.

REFERENCES

- Duan, Xudong, et al. "Quantitative understanding of lithium deposition-stripping process on graphite anodes of lithium-ion batteries." *Advanced Energy Materials* 13.10 (2023): 2203767.
- Attia, Peter M., et al. "'Knees' in lithium-ion battery aging trajectories." *Journal of The Electrochemical Society* 169.6 (2022): 060517.

